Coherent interference and diffraction in random waves

P.B. Smit [1] and T.T. Janssen[2]

[1] Environmental Fluid Mechanics, Faculty of Civil Engineering and Geosciences, Delft University of Technology, The Netherlands.

[2] Department of Geosciences, San Francisco State University, San Francisco, California, USA

Abstract

Wave fields traveling through a varying medium (e.g. topography, currents), can develop well-defined focal zones and caustics, where the wave field is highly coherent and wave statistics vary rapidly. However, the presence and evolution of such coherent structures in the wave field are not resolved in a quasi-homogeneous description of the wave field (e.g. the radiative transport equation), and a more general description of the wave statistics (and its evolution) is needed. In this work we demonstrate with numerical examples that, when using a (recently developed) transport equation for the second order inhomeogeneous wave statistics that accounts for cross-variance contributions, we can resolve coherent structures in wave fields such as those typically found in focal and diffraction zones. What this shows is, that in a statistical sense, diffraction is essentially an interference phenomenon that can be readily resolved if cross-phase information in the transport equations is retained.

1 Introduction

The dynamics and statistics of ocean waves are important e.g. for upper ocean dynamics (e.g. Craik & Leibovich, 1976), air-sea interaction, deep-ocean circulation (e.g. McWilliams & Restrepo, 1999), and coastal circulation and transport processes (e.g. Hoefel & Elgar, 2003). As a consequence, great advances have been made in our theoretical understanding of the evolution of wave statistics in the open ocean and near the coast, which in turn has led to the development of advanced and operational numerical wave prediction models (e.g. The WAMDI Group, 1988; Tolman, 1991; Komen *et al.*, 1994; Booij *et al.*, 1999; Wise Group, 2007). These models are based on the premise that the wave field can be described as a quasi-homogeneous and Gaussian random process, and are invariably based on some form of the radiative transfer equation, augmented with (parametrized) source terms to account for non-conservative processes and nonlinearity.

In the open ocean, where wave statistics evolve principally through the action of wind, dissipation (whitecapping), and cubic nonlinear effects, the assumption of quasi-homogeneous and Gaussian statistics is often reasonable. However, quasi homogeneous wave theory (radiative transfer equation) is particularly restrictive near the coast, where through the effects of medium variations (topography and currents), obstacles (e.g. coastal islands) and a transition to weakly dispersive wave motion, considerable deviations from homogeneity and Gaussian statistics can occur (e.g. Agnon & Sheremet, 1997; Herbers & Burton, 1997; Herbers *et al.*, 2003; Janssen *et al.*, 2008). To capture such wave coherent structures, be it introduced through medium variations or nonlinearity, requires the evaluation of additional correlators, and cannot be described by the evolution of (auto-)variance contributions alone. Efforts have been made to describe the evolution of inhomogeneous and/or non-Gaussian statistics for special cases (e.g. Agnon & Sheremet, 1997; Herbers *et al.*, 2003; Janssen *et al.*, 2008; Alber, 1978; Stiassnie *et al.*, 2008), but through additional assumptions (e.g. bandwidth, direction) such models are limited to certain special cases. A principal issue is the transport of (second- or higher-order) cross-correlations, which are needed to completely determine the wave statistics, but for which usually no conservation principles are available from the outset.

Recently Smit & Janssen (2011) considered the linear (Gaussian) case, and derived a new (approximate) transport equation (the Quasi-Coherent approximation) for inhomogeneous wave

statistics for wave fields of arbitrary bandwidth propagating through a variable medium. The model, that transports the Coupled Mode (or Wigner-Ville) spectrum, accounts for the coherent interference between wave components propagating at moderate angles, and can thus resolve rapid spatial variations in the wave statistics associated with wave interference. In the present work we briefly present the new theory (see Smit & Janssen, 2011, for details) and illustrate its implications through various numerical examples.

Thereto, we will start by introducing the Quasi-Coherent approximation and the coupled mode spectrum in §2 and relate the approximations to the Quasi-Homogeneous theory. In §3 we will consider two examples: 1) the coherent interference of two discrete of wave packages, and 2) wave diffraction through a narrow gap. What this shows is, that in a statistical sense, diffraction is essentially an interference phenomenon that can be readily resolved if cross-phase information in the transport equations is retained (as done here). Finally, we will discuss the properties, physical interpretation and origins of the cross-variance contributions in §4 and summarize our main results in §5.

2 The quasi-coherent approximation

To describe the evolution of coherent structures in random wave fields propagating through inhomogeneous media, Smit & Janssen (2011) derived an approximate transport equation for the second-order statistics of a (real) scalar, zero-mean random wave variable η (e.g. free surface elevation), as a function of the horizontal coordinates $\boldsymbol{x} = (x, y)$ and time t. To introduce this Quasi-Coherent (QC) approximation, we define a complex variable ζ, such that $\eta = \mathrm{Re}\{\zeta\}$ and its real and imaginary parts form a Hilbert transform pair (see e.g. Mandel & Wolf, 1995). Upon introducing the two-point correlator

$$\Gamma\left(\boldsymbol{\xi}, \boldsymbol{x}, t\right) = \frac{1}{2}\left\langle \zeta\left(\boldsymbol{x} + \frac{\boldsymbol{\xi}}{2}, t\right)\zeta^{*}\left(\boldsymbol{x} - \frac{\boldsymbol{\xi}}{2}, t\right)\right\rangle, \tag{1}$$

we define the coupled mode (CM) spectrum $\mathcal{E}$ as the Fourier transform of Γ to the separation coordinate $\boldsymbol{\xi}$,

$$\mathcal{E}\left(\boldsymbol{k}, \boldsymbol{x}, t\right) = \frac{1}{\left(2\pi\right)^{2}}\int \Gamma\left(\boldsymbol{x}, \boldsymbol{\xi}, t\right)\exp\left(-\mathrm{i}\boldsymbol{k}\cdot\boldsymbol{\xi}\right)\ d\boldsymbol{x}. \tag{2}$$

The Coupled-Mode (or Wigner-Ville) spectrum $\mathcal{E}$, thus captures the same statistical information as Γ, but is an intermediate representation between the physical and the spectral (wavenumber) domain. Assuming that the linear wave dynamics in a slowly varying medium admit plane wave solutions with a dispersion relation of the form

$$\omega = \Omega\left(\boldsymbol{k}, \boldsymbol{x}, t\right), \tag{3}$$

the evolution of the Coupled mode spectrum, and consequently the (complete) second-order wave correlation matrix, can be approximated with a transport equation that, upon defining $\boldsymbol{p} = [\boldsymbol{k}, \boldsymbol{x}]$, $\boldsymbol{q} = [\boldsymbol{x}, \boldsymbol{k}]$, is given by (Smit & Janssen, 2011)

$$\frac{\partial \mathcal{E}}{\partial t} + \mathcal{C}_{m}\frac{\partial \mathcal{E}}{\partial q_{m}} + \mathcal{C}_{m,n,o}\frac{\partial^{3}\mathcal{E}}{\partial q_{m}\partial q_{n}\partial q_{o}} = 0, \tag{4}$$

where the coefficients $\mathcal{C}$ are defined as

$$\mathcal{C}_{m} = -s_{m}\frac{\partial \Omega}{\partial p_{m}} \qquad\qquad \mathcal{C}_{m,n,o} = s_{m}s_{n}s_{o}\frac{1}{24}\frac{\partial^{3}\Omega}{\partial p_{m}\partial p_{n}\partial p_{o}}. \tag{5}$$

The approximate expression (4) describes the evolution of the second-order wave statistics while accounting for the presence of coherent structures in the wave field. Since it is the result of a truncated series approximation around the homogeneous state (at the third order, see Smit & Janssen, 2011), we refer (4) as the Quasi-Coherent approximation, and note that it is accurate for coherent interference between wave components propagating at moderate ($< 30^{\circ}$) mutual angles.

The QC approximation describes the wave statistics in terms of the CM spectrum, which from its definition appears similar to the variance density (or Power) spectrum (e.g. Komen et al., 1994); indeed the local wave variance $\mathcal{V}(\boldsymbol{x},t)$ at $(\boldsymbol{x},t)$ is a marginal distribution of $\mathcal{E}$, as in

$$\mathcal{V}(\boldsymbol{x},t) = \int \mathcal{E}(\boldsymbol{k},\boldsymbol{x},t)\, d\boldsymbol{k}. \tag{6}$$

Despite these similarities, the CM spectrum cannot be interpreted as a variance density spectrum (see e.g. Janssen & Claasen, 1985). The principle difference is that the CM spectrum constitutes a complete representation of the second-order statistics, including possible interference terms that are associated with rapid variations in the statistics (e.g. Janssen *et al.*, 2008). In particular, although the CM spectrum is a real function, it is not generally positive, which in general precludes an interpretation as a variance density spectrum.

However, in the limit where the wave field is Quasi-Homogeneous the CM spectrum does reduce to a variance density function. In this case, we can neglect all but the first order terms on the LHS of (4), which then reduces to the radiative transport equation. This shows that equation (4) contains QH theory as a special case, and is a natural extension of the radiative transfer equation in areas where the statistics undergo potentially rapid (intra-wave scales) variations due to the presence of inhomogeneities (coherent wave interference) in the wave field. In the context of ocean waves, such inhomogeneities can be induced for instance by medium variations (seafloor bathymetric features and variable currents). In the remainder of this paper we will demonstrate that the inclusion of cross-variance contributions is vital for a correct representation of the wave statistics in focal and diffraction zones.

3 Coherent interference in focal and diffraction zones

3.1 Coherent Gaussian packets

A simple example that illustrates how the inclusion of wave coherence can introduce rapid spatial variations in the wave statistics can be constructed by considering a wave field for which at $t = t'$, a realization of the sea surface can be represented as a superposition of two coherent Gaussian-shaped wave packets, each with a complex amplitude A_m and carrier wave number $\boldsymbol{k}_m$, written as

$$\zeta(\boldsymbol{x}, t = t') = A_1 \exp\left(-\alpha |\boldsymbol{x}|^2 + \mathrm{i}\boldsymbol{k}_1 \cdot \boldsymbol{x}\right) + A_2 \exp\left(-\alpha |\boldsymbol{x}|^2 + \mathrm{i}\boldsymbol{k}_2 \cdot \boldsymbol{x}\right). \tag{7}$$

To obtain the coupled mode spectrum at $t = t'$, we take the Fourier transform with respect to $\boldsymbol{\xi}$ of the two-point correlator Γ, so that

$$\begin{aligned}\mathcal{E}_{t'}(\boldsymbol{k},\boldsymbol{x}) = \frac{1}{4\pi\alpha}\exp\left[-2\alpha|\boldsymbol{x}|^2\right]\Bigg\{&\langle A_1 A_1^*\rangle \exp\left[-\frac{1}{2\alpha}|\boldsymbol{k}-\boldsymbol{k}_1|^2\right] \\ &+ \langle A_2 A_2^*\rangle \exp\left[-\frac{1}{2\alpha}|\boldsymbol{k}-\boldsymbol{k}_2|^2\right] \\ &+ \exp\left[-\frac{1}{2\alpha}\left|\boldsymbol{k}-\frac{1}{2}(\boldsymbol{k}_1+\boldsymbol{k}_2)\right|^2\right]\left(\langle A_1 A_2^*\rangle \exp\left[-\mathrm{i}(k_1-k_2)\cdot\boldsymbol{x}\right] + \mathrm{C.C}\right)\Bigg\}\end{aligned} \tag{8}$$

The first two terms on the RHS of (8) correspond to the auto-variance contributions of the individual packets, whereas the last term represents the rapid spatial interference when the two packets are coherent. The inclusion of such interference terms is what differentiates the coupled mode spectrum from the Variance density spectrum, which only accounts for the auto-variance contributions. These interference terms are located midway between the two corresponding auto-terms (at $\frac{1}{2}(\boldsymbol{k}_1 + \boldsymbol{k}_2)$), might become negative, and can vary on potentially much faster spatial scales. Consequently, due to interference, the wave statistics can vary on scales comparable to a typical wavelength, even if the associated auto-terms vary slowly (or not at all).

To illustrate the difference between the QC and QH approximation we shall consider the time evolution of a two-packet system which at $t = t'$ is described by (8). Assuming that the dispersion

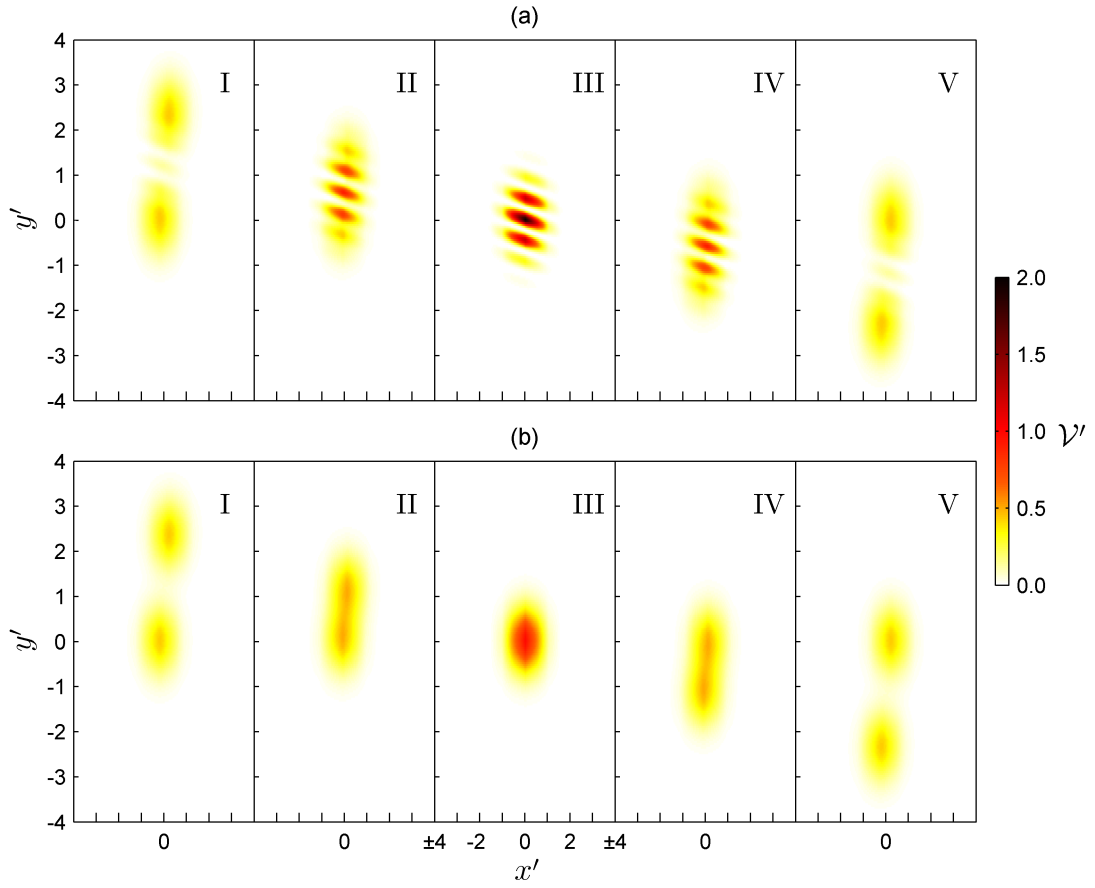

Figure 1: Snapshots of normalized wave variance (normalization by a^2) of two-packet interference example. The wave variance is shown at discrete times t_{I-V}, starting at $t_I = 110L_p/v_x$ (left panels) increasing in time (from left to right) in intervals of $\Delta t = 20L_p/v_x$. Top panel (a) shows evolution for the QC-approximation (9); bottom panel (b) shows the evolution according to QH theory. The x' and y' denote the horizontal coordinates normalized with $6L_p$.

relation is given by the deep-water relation, the QC approximation (4) decouples in spectral space (since $\nabla_{\boldsymbol{x}}\Omega = 0$) so that, using Fourier transforms, the solution at an arbitrary time t is given by (Smit & Janssen, 2011)

$$\mathcal{E}(\boldsymbol{k},\boldsymbol{x},t) = \frac{1}{(2\pi)^2}\iint d\boldsymbol{u}d\boldsymbol{x}'\,\mathcal{E}_{t'}\exp\left[-\mathrm{i}\boldsymbol{u}\cdot\boldsymbol{x}' + \mathrm{i}\boldsymbol{u}\cdot\boldsymbol{x} - \mathrm{i}(t-t')w(\boldsymbol{k},\boldsymbol{u})\right] \tag{9}$$

where

$$w(\boldsymbol{k},\boldsymbol{u}) = u_1\frac{\partial\Omega}{\partial k_1} + u_2\frac{\partial\Omega}{\partial k_2} + \frac{1}{24}u_1^3\frac{\partial^3\Omega}{\partial k_1^3} + \frac{1}{24}u_2^3\frac{\partial^3\Omega}{\partial k_2^3} + \frac{1}{8}u_1u_2^2\frac{\partial^3\Omega}{\partial k_1(\partial k_2)^2} + \frac{1}{8}u_2u_1^2\frac{\partial^3\Omega}{\partial k_2(\partial k_1)^2} \tag{10}$$

The Quasi-Homogeneous solution can be obtained in a similar way from equation (9), by only accounting for the first two terms on the RHS in equation (10), and neglecting the cross-variance contributions to the spectrum in the initial conditions.

We adopt a reference frame that, relative to the medium, travels with a fixed velocity $\boldsymbol{v}$ and assume deep water conditions so that the dispersion relation becomes $\Omega(\boldsymbol{k}) = \sqrt{g|\boldsymbol{k}|} + \boldsymbol{k}\cdot\boldsymbol{v}$. The

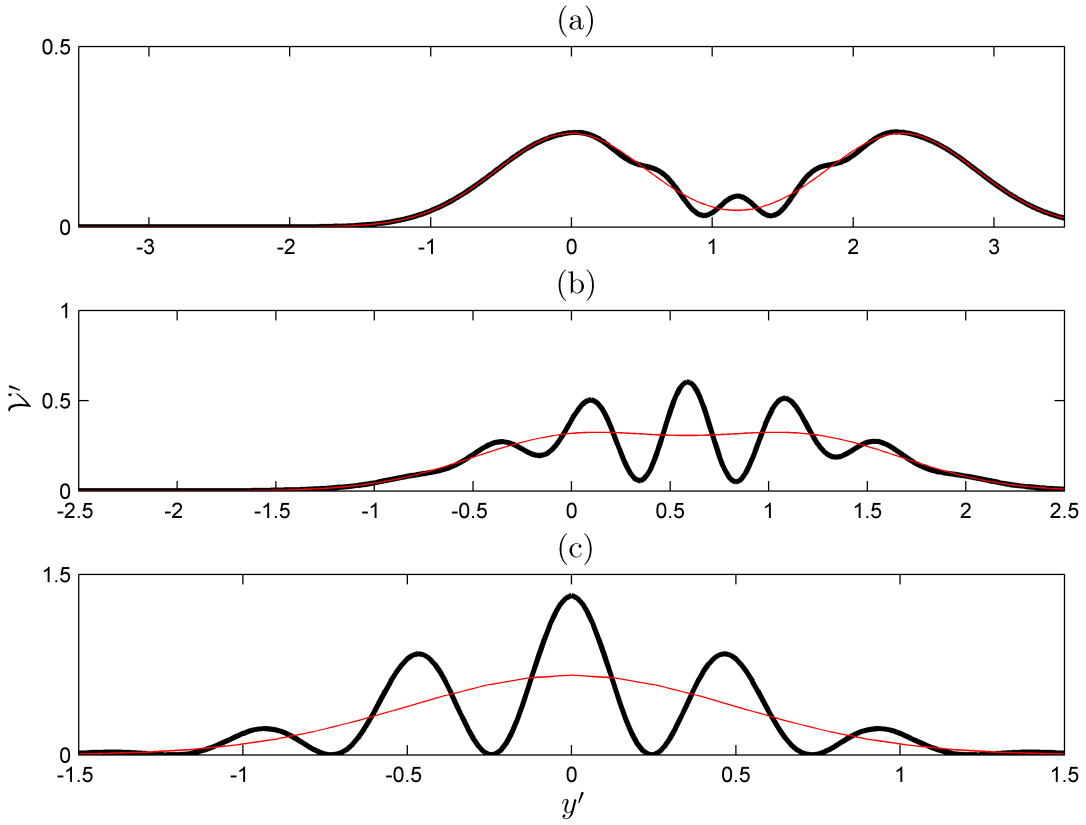

Figure 2: Cross-sections (at $x' = 0$) of normalized wave variance of the two-packet interference example. The wave variance is shown at discrete times t_{I-V}, starting at t_I (a) and increasing in time (from left to right). Comparison between the QC-approximation (Solid line), and the evolution according to QH theory (Thin red line). Normalization of vertical and horizontal scales and discrete times as in figure 1. Note that the horizontal and vertical range can vary between panels.

two packets (with equal amplitudes $|A| = a$ and carrier wavelength L_p) travel at a mutual angle of 20 degrees, with one packet traveling along the positive x-axis. We set $\alpha = \frac{1}{36}L_p^{-2}$, so that a characteristic length scale of the packets is roughly six wave lengths, let the coordinate frame travel at the mean group velocity along the x axis $v_x = \frac{1}{2}\bar{k}_x k_p^{-1}\sqrt{g/k_p}$ (with $k_p = 2\pi L_p^{-1}$, $\bar{\boldsymbol{k}}$ is the mean carrier wave number and $v_y = 0$), and set $t' = 150L_p/v_x$. To evaluate (8) numerically, each packet is calculated individually on a discrete equidistant $\boldsymbol{k}$-mesh using thirty points in each direction with a mesh-size of $\Delta k = \sqrt{\alpha}/5$. The Fourier integrals are approximated using a Fast Fourier Transform on a discrete array $[-31 \ldots 31]\,\Delta u$ for u_1 and u_2 with $\Delta u = \sqrt{\alpha}/5$, and the result is then interpolated to a discrete 241×241 $\boldsymbol{x}$-mesh centered at the origin with mesh-size $\Delta x = \Delta y = L_p/5$.

If the two packets are coherent (and in phase at $t = t'$), the evolution of the wave system (using the QC approximation) is characterized by convergence and interference of the wave packets, followed by de-focusing and divergence, after which the packets emerge unchanged (figure 1a and 2). In contrast, the wave packet evolution as represented by QH theory (figures 1b and 2), which assumes that all contributions are independent, is dramatically different; in particular, the interference pattern at $t = t_{III}$ is absent entirely, as a result of the inability of QH theory to account for cross-variance contributions.

That the QC approximation gives fundamentally different results is also apperent when we evalute the coupled mode spectrum at different time instances along the line $\boldsymbol{x'} = 0$ (figure 3a). The auto-variance contributions at $k'_y = 0$ (t_I to t_V) and $k'_y = -0.35$ (t_{III}), associated with the wave packets traveling at 0 and -20 degrees respectively, essentially comprise what would be the variance density spectrum. However, since the CM spectrum accounts for the inter-mode coupling it contains an additional interference peak which travel along a ray midway between the rays of the

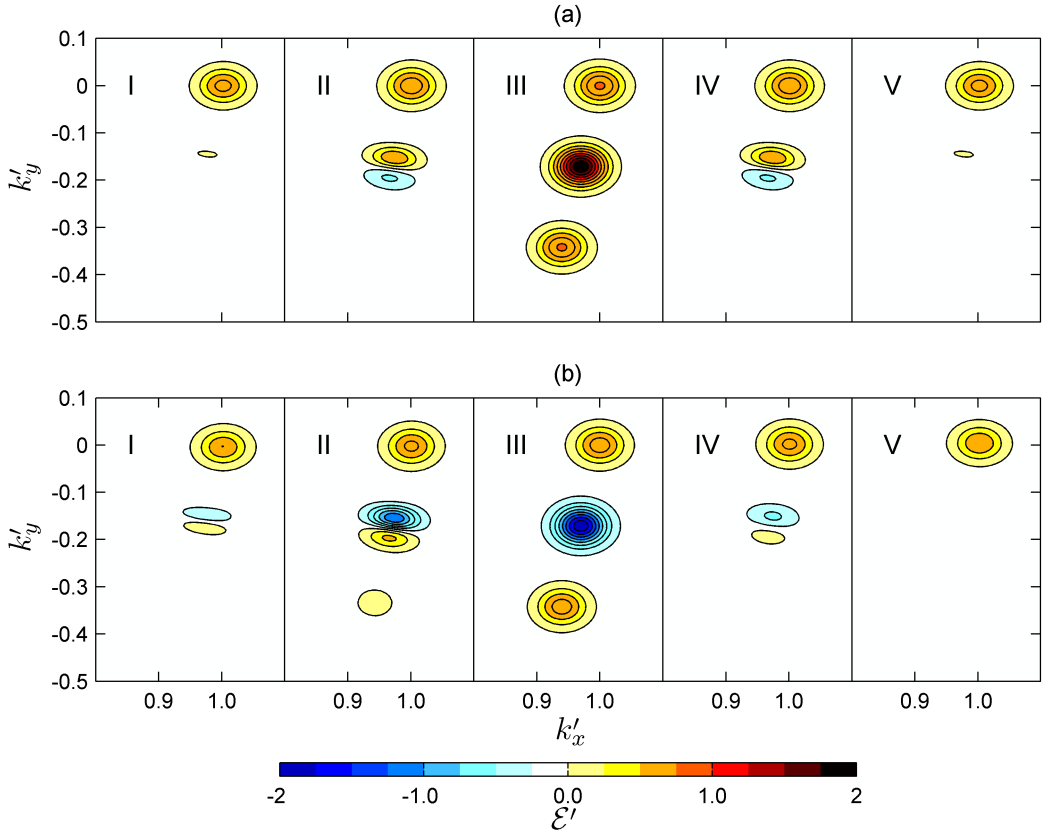

Figure 3: Spectral evolution of the two-packet interference example evaluated at $(x', y') = 0$ (a) and $(x', y') = (0, \frac{1}{4})$ (b) for t_{I-V} (times as defined in caption figure 1). The spectral coordinates k'_x and k'_y are normalized with k_p and spectra are normalized with the peak contribution of an individual packet $(4\pi\alpha)^{-1}$.

auto-variance contributions, and therefore manifests itself most prominently between t_{II} to t_{IV}, when the two packets have converged. This spectral interference term captures the rapid spatial oscillations of the wave statistics associated with coherent interference patterns in the physical domain (figure 1a). This fast-scale variability is also seen in the spectral domain when the spectra are evaluated at a slightly offset location (compare panels a and b in figure 3). Note that the wave packets in this example do not 'interact' with each other in the usual sense. Their interference is completely determined a-priori by the inclusion of interference peaks in the initial condition.

3.2 Wide angle diffraction

A well-known example of how the initial conditions, including information regarding the coherency between wave components propagating in various directions, fully determines the wave field evolution (and its statistics), is that of diffraction around a thin barrier. To illustrate how the evolution of a diffracted wave field can be described in a purely statistical framework, we apply our QC approximation to a classic example of diffraction through a gap (extending over $-G_1 < y < G_2$), in an otherwise rigid, but fully absorbing barrier (situated at $x = 0$). Apart from the obstacle, the medium is uniform and the incident wave field in the half-plane $x < 0$ is stationary and known.

For a stationary field in an homogeneous medium the Fourier transform of the CM spectrum to $\boldsymbol{x}$ can only contain contributions for wavenumbers $\boldsymbol{k}, \boldsymbol{u}$ that are perpendicular to one-another ($\boldsymbol{k}\cdot\boldsymbol{u} = 0$, see Smit & Janssen, 2011). Hence, if the field components are restricted to contributions traveling in (say) the positive x direction, and given the CM spectrum $\mathcal{E}_{0^+}$ along the line $x = 0$, the solution in the half plan $x \geq 0^+$, using $u_x = -u_y k_y k_x^{-1}$, can be written in the form (see Smit

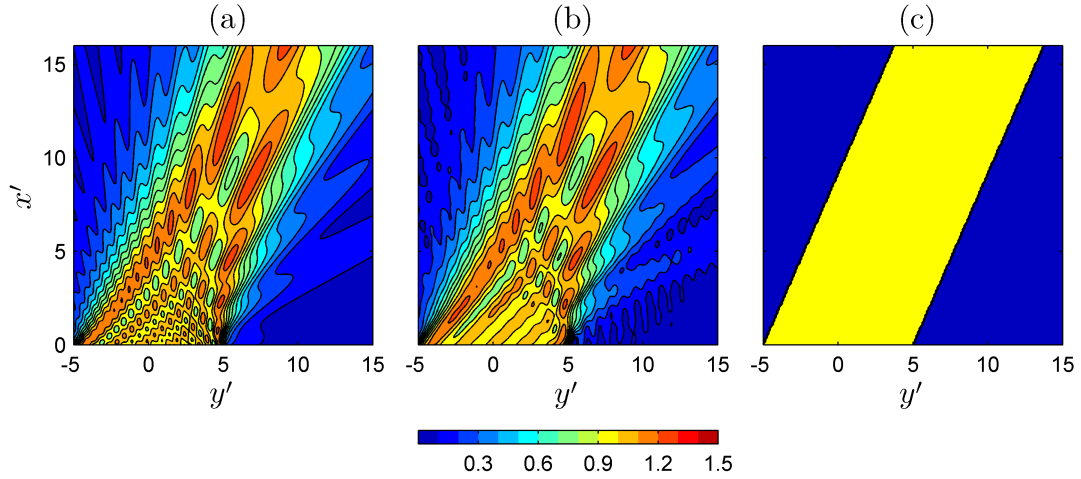

Figure 4: Contours of the normalized wave height $H' = \sqrt{\mathcal{V}/\mathcal{V}_0}$ (where $\mathcal{V}_0$ is the variance of the incident waves) behind a breakwater gap (top panels). Panel(a) corresponds to an analytic solution (Penney & Price, 1952), panel (b) to the Quasi-Coherent solution and panel (c) represents the Quasi-Homogeneous solution. The incident wave field consists of uni-directional waves (with $\theta_0 = 30^\circ$), with a peak angular frequency of $\omega_p = \pi$ rad/s, $k_p h = 1.2$ and a narrow-band Gaussian-shaped frequency distribution with characteristic width of $\Delta\omega = \frac{1}{100}\omega_p$. The horizontal coordinates (x', y') are normalized with the peak wavelength.

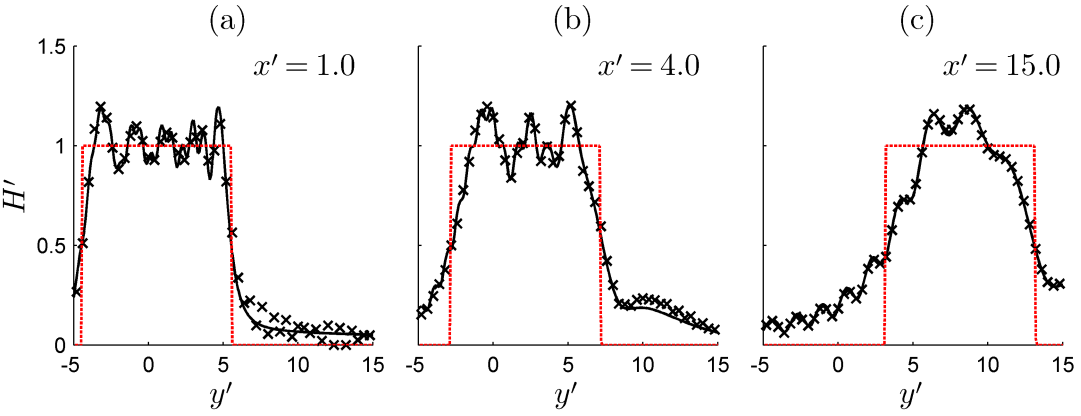

Figure 5: Lateral cross-sections of of the normalized wave height H' behind a breakwater gap along $x' = 1$ (a), $x' = 4$ (b) and $x' = 15$ (c). Shown are the analytic solution (solid line), the QC approximation (cross markers) and the QH solution (thin red line). Incident wave field and coordinates as in figure **??**.

& Janssen, 2011)

$$\mathcal{E}(\boldsymbol{k}, \boldsymbol{x}) = \frac{1}{(2\pi)^2} \iint \mathcal{E}_{0^+} \exp\left(-\mathrm{i}u_y y' + \mathrm{i}u_y y - \mathrm{i}u_y k_y k_x^{-1} x\right) dy' du_y, \tag{11}$$

which, upon taking the spatial derivative ∂_x on both sides, becomes

$$\partial_x \mathcal{E} = -\frac{k_y}{k_x} \partial_y \mathcal{E}, \qquad \text{when} \quad x \geq 0^+, k_x > 0. \tag{12}$$

Equation (12) implies that the solution for stationary fields in homogeneous media is invariant along the rays of Geometric optics, and consequently that the evolution of the wave field is implied by the initial condition (at $x = 0$). Hence, the wave statistics behind the breakwater gap, including possible coherent interference between components, are obtained from (11) once the transfer function between the incident wave field and the scattered spectrum at $x = 0^+$ is known.

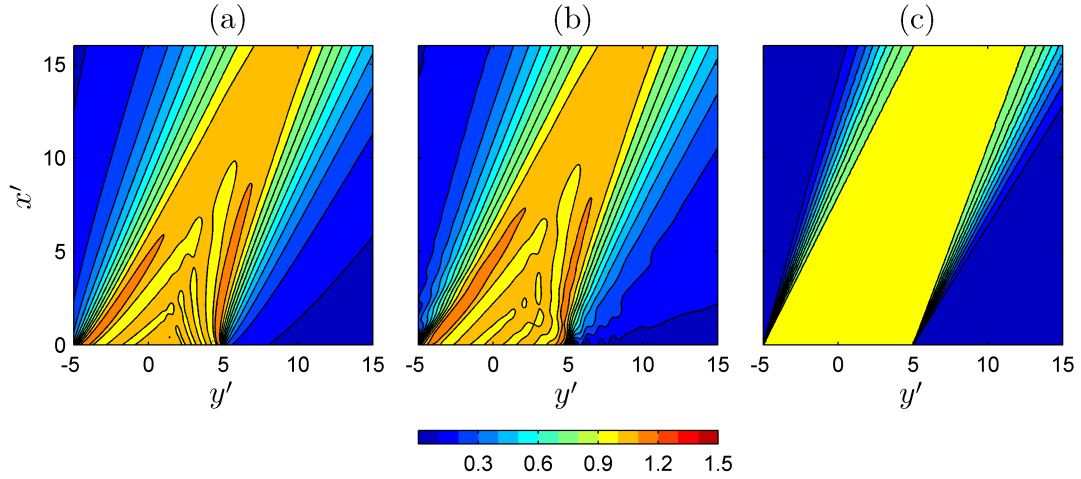

Figure 6: Contours of the normalized wave height $H' = \sqrt{\mathcal{V}/\mathcal{V}_0}$ (where $\mathcal{V}_0$ is the variance of the incident waves) behind a breakwater gap (top panels). Panel(a) corresponds to an analytic solution (Penney & Price, 1952), panel (b) to the Quasi-Coherent solution and panel (c) represents the Quasi-Homogeneous solution. The incident wave field consists of directionally spread waves (raised cosine distribution with $\theta_0 = 30^\circ$), with a peak angular frequency of $\omega_p = \pi$ rad/s, $k_p h = 1.2$ and a Gaussian-shaped frequency distribution with characteristic width of $\Delta\omega = \frac{1}{10}\omega_p$. The horizontal coordinates (x', y') are normalized with the peak wavelength.

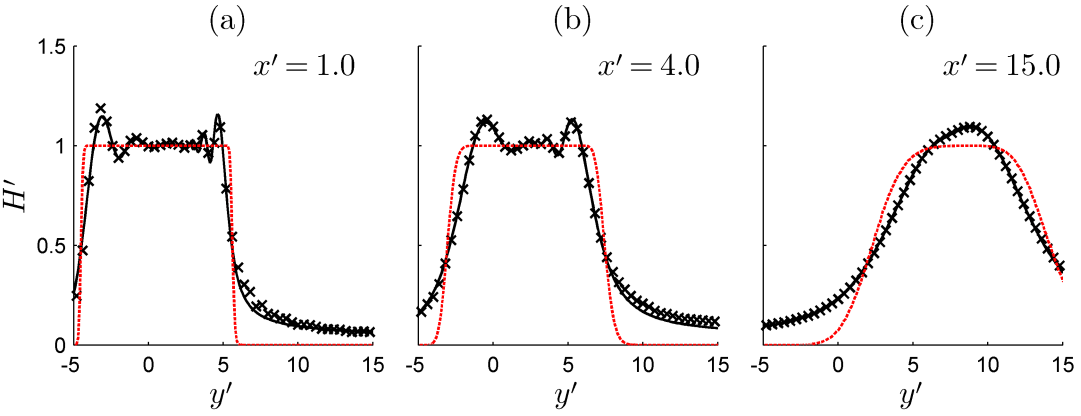

Figure 7: Lateral cross-sections of of the normalized wave height H' behind a breakwater gap along $x' = 1$ (a), $x' = 4$ (b) and $x' = 15$ (c). Shown are the analytic solution (solid line), the QC approximation (cross markers) and the QH solution (thin red line). Incident wave field and coordinates as in figure **??**.

Using the Kirchhoff, or physical optics, approximation (e.g. Born & Wolf, 1999, p. 422) we can derive an approximate boundary condition just behind the barrier ($x = 0^+$) (see Janssen *et al.*, 2008), which, in terms of the CM spectrum,becomes (see Smit & Janssen, 2011)

$$\mathcal{E}_{0^+}(\boldsymbol{k}, y) = \int du_y \begin{cases} \mathcal{S}\left|\frac{\partial\widehat{\omega}}{\partial k_x}\right| \exp\left(\mathrm{i}u_y y\right) & \text{if } k_x > 0 \ \left|k_x \mp \frac{k_y u_y}{2k_x}\right| \geq 0 \\ 0 & \text{elsewhere} \end{cases}, \tag{13}$$

where

$$\mathcal{S}(\boldsymbol{k}, y) = \frac{1}{\pi^2} \int dk'_y \left\{ S_0\left(\widehat{\omega}, k'_y\right) \exp\left(-\mathrm{i}u_y G_\Delta\right) \frac{|\boldsymbol{k}|^2 + u_y^2\left(1 + k_y^2 k_x^{-2}\right) - (k'_y)^2}{k_x^2 - \frac{1}{4}k_x^{-2}k_y^2 u_y^2} \right.$$
$$\left. \frac{\sin\left((k'_y - k_y - u_y/2)G_m\right)}{(k_y + u_y/2)} \frac{\sin\left((k'_y - k_y + u_y/2)G_m\right)}{(k_y - u_y/2)} \right\}. \tag{14}$$

Here $G_\Delta = (G_2 - G_1)/2$, $G_m = (G_1 + G_2)/2$, $S_0(\omega, k_y)$ is the variance density spectrum in the region $x < 0$, expressed in terms of the angular frequency and lateral wavenumber k_y, and $\widehat{\omega}$ is given by

$$\widehat{\omega}(\boldsymbol{k}, u_y) = \Omega(\boldsymbol{k}) + \frac{u_y^2 k_y^2}{4k_x^2}\frac{\partial^2\Omega}{\partial k_x^2} - \frac{1}{4}u_y^2\frac{\partial^2\Omega}{\partial k_y^2} + \frac{u_y^2 k_y}{2k_x}\frac{\partial^2\Omega}{\partial k_x \partial k_y} \tag{15}$$

To illustrate that the QC approximation accurately represents wave fields in diffraction zones, we compare equation (11), initialized with (13), to an analytic solution (Penney & Price, 1952), and a Quasi-Homogeneous solution[1], for a gap configuration of $G_1 = G_2 = 5L_p$, where L_p is the wavelength at the peak of $\mathcal{S}_0$. The incident wavefield is assumed to have a Gaussian frequency distribution and a raised cosine directional distribution

$$S_0(\omega, \theta) = \frac{\mathcal{V}_0 D(\theta)}{\sqrt{2\pi}\Delta\omega}\exp^{\frac{-(\omega-\omega_p)^2}{2(\Delta\omega)^2}} \qquad D(\theta) = \begin{cases} \frac{\Gamma(\frac{1}{2}m+1)}{\sqrt{\pi}\Gamma(\frac{1}{2}m+\frac{1}{2})}\cos^m(\theta-\theta_0) & |\theta| < \pi/2 \\ 0 & \text{elsewhere} \end{cases} \tag{17}$$

where $\mathcal{V}_0$ is the variance, ω_p the angular frequency at the peak, $\Delta\omega$ a characteristic width and θ_0 the mean wave direction.

When we consider a narrow-banded, uni-directional wave field ($\Delta\omega/\omega_p = 1/100\,,\, m \to \infty$), the agreement between the analytic result and the QC approximation is excellent (figures 4 and 5) for distances greater than about 4 wavelengths behind the barrier ($x/L_p > 4$), which confirms that (4) accurately describes diffracted fields in the intermediate to far-field. In the near-field, the approximation is less accurate, in part due to the lack of high-frequency spatial modes, but principally due to the omission of evanescent modes (especially in the region $x/L_p < 1$), and the use of an approximate (Kirchhoff) boundary condition (see e.g. Stamnes, 1986). Evidentially, compared to the QH solution, the QC approximation is a radical improvement, mainly because the assumption of mutually independent spectral constituents prevents the inclusion of the coherent scattering by the gap in the boundary condition, so that only the sheltering effect is represented in the QH solution.

For directionally spread waves with a broader bandwidth ($\Delta\omega/\omega_p = 1/10\,,\, m = 200$), the fast scale spatial oscillations in the variance are smoothed so that the variations in the wave statistics become more gradual, and the correspondence in the region $x/L_p < 4$ between the QC approximation and the analytical solution generally improves (figures 6 and 7). The stochastic approach presented here is more suitable for these type of conditions, where the wave statistics vary on an intermediate scale, so that a theory that accounts for the coherence between components that propagate at moderate mutual angles is necessary (figures 6 and 7), and provides sufficiently accurate results.

4 Discussion

The principle difference between the variance density spectrum (e.g. Komen *et al.*, 1994) and the coupled mode spectrum is that the latter includes interference (cross-covariance) terms, and thus forms a more complete representation of the wave statistics. In this section we shall briefly discuss the properties and physical interpretation of the cross-variance terms, and address how such terms may originate from initially quasi-homogeneous conditions by interaction with the topography.

The two-packet example (7) in section §3.1 illustrated that, when the contributions are mutually coherent, an additional cross-variance peak appears in between the two auto-variance contributions, that accounts for the rapid spatial variations in the wave statistics. In general, such cross-variance contributions are always located midway (spatially and spectrally) between the associated auto-variance contributions (Hlawatsch & Flandrin, 1997), are generally oscillatory, and

[1] For the Quasi-Homogeneous solution we simply replace (13) with

$$\mathcal{E}_{0^+}(\boldsymbol{k}, y) = \begin{cases} S_0(\boldsymbol{k}) & \text{if } -G_1 < y < G_2 \\ 0 & \text{elsewhere} \end{cases}\,, \tag{16}$$

where $S_0(\boldsymbol{k})$ is the variance density spectrum in the region $x < 0$. Hence, what we refer to as the QH solution is essentially a Geometric optics approximation.

can become negative. Furthermore, since they do not directly correspond to a field component, they do not carry energy themselves. Instead, these terms carry additional (cross-phase) information that determines how the energy of the wave field is distributed between kinetic and potential energy. In particular, if a wave field is statistically homogeneous (without coherent interferences), wave energy is equipartitioned, so that knowledge of the potential energy (the auto-variance contributions) suffices. In a wave field that undergoes coherent interference, information on the distribution of potential and kinetic energy is required to fully characterize the wave field statistics. Our examples show that, by including such information, the coupled mode spectrum can represent the rapidly varying wave statistics as found in focal and diffraction zones.

However, in the present work this information was essentially already contained within the initial conditions (§3.1), or prescribed at the boundary (§3.2), and we have not yet discussed, or considered, the generation (and evolution) of such interference contributions. Physically, coherent interference contributions can be induced by medium variations. In the particular case of ocean waves, this occurs in areas where currents and sea-floor topography are strongly two-dimensional, such as can be found in coastal areas and on the continental shelves. For example, the refractive scattering of a narrow-band wave field impinging on a shoal or canyon can result in a focal zone where cross-correlations non-collinear components are critical to resolve the rapid variations in wave statistics in such regions (e.g. Magne *et al.*, 2007). In such regions, which are not uncommon in coastal areas, an energy balance model can be inadequate (e.g. O'Reilly & Guza, 1991) and a quasi-coherent approach is physically more realistic. This will be discussed in more detail in a following paper, where we apply the present theory to recent field observations of refraction and scattering of waves over a nearshore canyon in Southern California (Thomson *et al.*, 2007; Magne *et al.*, 2007).

5 Conclusions

In this paper we have considered the implications of a new approach (the Quasi-Coherent approximation) to the stochastic modeling of ocean waves of arbitrary bandwidth that, in contrast to Quasi-Homogeneous theory, accounts for the generation and evolution of coherent interference between wave components, and reduces to Quasi-Homogeneous theory if interference terms are negligible. We have illustrated that, particularly for narrow-banded waves, the inclusion of cross-variance contributions can lead to significant differences in the wave statistics in focal and diffraction zones, and verified, by comparison to an analytic solution, that the Quasi-Coherent approximation can accurately resolves the interference patterns associated with crossing waves. Our results suggest that the Quasi-Coherent theory developed here is suitable for the evolution of wave statistics in the presence of caustics and in refractive focal zones, which is of interest in the study of wave statistics (and anomalies therein) in areas of two-dimensional medium variations, particularly in coastal areas.

Acknowledgments

This research is supported by the U.S. Office of Naval Research (Coastal Geosciences Program and Physical Oceanography Program) and by the National Oceanographic Partnership Program. The authors thank Leo Holthuijsen whose continuing support made it possible for PBS to pursue this research.

References

Agnon, Y. & Sheremet, A. 1997 Stochastic nonlinear shoaling of directional spectra. *J. Fluid Mech.* **345**, 79–99.

Alber, I. E. 1978 The effects of randomness on the stability of two-dimensional surface wavetrains. *Proc.R.Soc.London* **363** (1715), 525–546.

Booij, N., Ris, R. C. & Holthuijsen, L. H. 1999 A third-generation wave model for coastal regions 1. model description and validation. *J. Geophys. Res.* **104**, 7649–7666.

Born, M. & Wolf, E. 1999 *Principles of Optics*, 7th edn. Cambridge: Cambridge university press.

Craik, A. D. D. & Leibovich, S. 1976 A rational model for langmuir circulations. *J. Fluid. Mech.* **73**, 401–426.

Herbers, T. H. C. & Burton, M. C. 1997 Nonlinear shoaling of directionally spread waves on a beach. *J. Geophys. Res.* **102**, 21,101–21,114.

Herbers, T. H. C., Orzech, Mark, Elgar, Steve & Guza, R. T. 2003 Shoaling transformation of wave frequency-directional spectra. *J. Geophys. Res.* **108** (C1), 3013.

Hlawatsch, F. & Flandrin, P. 1997 The interference structure of the wigner distribution and related time-frequency signal representations. In *The Wigner Distribution - Theory and Applications in Signal Processing* (ed. W. Mecklenbrauker & F. Hlawatsch), pp. 59–133. Amsterdam: Elsevier.

Hoefel, F. & Elgar, S. 2003 Wave-induced sediment transport and sandbar migration. *Science* **299**, 1885–1887.

Janssen, A. & Claasen, T. 1985 On positivity of time-frequency distributions. *Acoustics, Speech and Sig. Proc., IEEE Trans.* **33** (4), 1029–1032.

Janssen, T. T., Herbers, T. H. C. & Battjes, J. A. 2008 Evolution of ocean wave statistics in shallow water: Refraction and diffraction over seafloor topography. *J. Geophys. Res.* **113** (C3), C03024.

Komen, G.J., Cavaleri, L., Donelan, M., Hasselmann, K., Hasselmann, S. & Janssen, P.A.E.M. 1994 *Dynamics and Modelling of Ocean Waves*. Cambridge: Cambridge Univ. Press.

Magne, R., Belibassakis, K. A., Herbers, T. H. C., Ardhuin, F., O'Reilly, W. C. & Rey, V. 2007 Evolution of surface gravity waves over a submarine canyon. *J. Geophys. Res.* **112** (C1), C01002.

Mandel, L. & Wolf, E. 1995 *Optical coherence and Quantum Optics*. Cambridge: Cambridge Univ. Press.

McWilliams, J. C. & Restrepo, J. M. 1999 The wave-driven ocean circulation. *Oceanogr* **29**, 2523–2540.

O'Reilly, W. C. & Guza, R. T. 1991 Comparison of spectral refraction and refraction-diffraction wave models. *J. Wat. Port Coast. Ocean Eng.* **117** (3), 199–215.

Penney, W. G. & Price, A. T. 1952 Part i. the diffraction theory of sea waves and the shelter afforded by breakwaters. *Proc.R.Soc.London* **244** (882), 236–253.

Smit, P.B. & Janssen, T.T 2011 Coherent structures in random waves. *Manuscript submitted for publication* .

Stamnes, J.J. 1986 *Waves in focal regions: propagation, diffraction, and focusing of light, sound, and water waves*. Boston: A. Hilger.

Stiassnie, M., Regev, A. & Agnon, Y. 2008 Recurrent solutions of alber's equation for random water-wave fields. *J. Fluid Mech.* **598**, 245–266.

The WAMDI Group 1988 The wam model - a third generation ocean wave prediction model. *J. Phys. Oceanogr* **18** (12), 1775–1810.

Thomson, J., Elgar, S., Herbers, T. H. C., Raubenheimer, B. & Guza, R. T. 2007 Refraction and reflection of infragravity waves near submarine canyons. *J. Geophys. Res.* **112**.

Tolman, H. L. 1991 A third-generation model for wind waves on slowly varying, unsteady, and inhomogeneous depths and currents. *J. Phys. Oceanogr* **21** (6), 782–797.

Wise Group 2007 Wave modelling - the state of the art. *Progress In Oceanogr.* **75** (4), 603–674.